Journal of Helminthology

cambridge.org/jhl

Eurytrema coelomaticum: updated morphology of adult worms using advanced microscopy experiments

K.G. Leite[1,*], E.J. Lopes-Torres[1,*], J.G.R. Souza[2], R.H. Neves[1], D.C. Gomes[3] and J.R. Machado-Silva[1]

[1]Laboratório de Helmintologia Romero Lascasas Porto, Departamento de Microbiologia, Imunologia e Parasitologia, Faculdade de Ciências Médicas, Centro Biomédico, Universidade do Estado do Rio de Janeiro, Av. Prof. Manoel de Abreu 444/5° andar, Vila Isabel, 20511-070, Rio de Janeiro, Brazil; [2]Laboratório de Biologia e Parasitologia de Mamíferos Silvestres Reservatórios, FIOCRUZ, Av. Brasil 4365, Manguinhos 21040-900, Rio Janeiro, Brazil and [3]Laboratório de Helmintos Parasitos de Vertebrados, Instituto Oswaldo Cruz, FIOCRUZ Pavilhão Cardoso Fontes 3° andar, Av. Brasil, 4365, Manguinhos, 21040-900, Rio de Janeiro, Brazil

Research Paper

*These authors contributed equally to this work.

Cite this article: Leite KG, Lopes-Torres EJ, Souza JGR, Neves RH, Gomes DC, Machado-Silva JR (2020). *Eurytrema coelomaticum*: updated morphology of adult worms using advanced microscopy experiments. *Journal of Helminthology* **94**, e122, 1–9. https://doi.org/10.1017/S0022149X19001135

Received: 10 September 2019
Revised: 13 November 2019
Accepted: 23 December 2019

Key words:
Eurytrema coelomaticum; morphology; confocal microscopy; scanning electron microscopy; cryofracture

Author for correspondence:
J.R. Machado-Silva, E-mail: jrmasilva@gmail.com

Abstract

Eurytrema coelomaticum is a digenean flatworm of ruminants that is the causative agent of eurytrematosis, a disease of veterinary health concern. Although modern techniques of morphological analysis have provided new insights about the morphology and anatomy of parasitic helminths, most studies on *E. coelomaticum* adults are based on conventional light microscopy. In the present study, a combined approach using brightfield, fluorescence, confocal and scanning electron microscopies (SEMs), together with the cryofracture technique, have updated morphological data on *E. coelomaticum* recovered from cattle in Rio de Janeiro State, Brazil. Light microscopy confirmed the presence of several structures present in the current description, such as suckers, pharynx, oesophagus, intestinal bifurcation and the cirrus-sac. Fluorescence stereomicroscopy revealed for the first time the cubic crystal protein inclusions in the forebody, which were further detailed by confocal and SEMs. Confocal microscopy provided detailed information of the muscular architecture associated with the attachment structures (suckers), digestive system (pharynx and oesophagus), egg-forming complex (ovary, Mehlis' gland and Laurer's canal) and male reproductive system, which are similar to those found in other digenean flukes. SEM images of cryofractured parasites showed mucus and developing eggs within uterine loops. It was demonstrated that the combination of advanced tools generated complementary information, confirming the importance of experimental morphology in parasitology. Therefore, the knowledge of the adult structural organization of *E. coelomaticum* was improved and this work has contributed to propose new morphological criteria to evaluate the effects of antiparasitic drugs on flukes of medical and veterinary importance.

Introduction

Eurytrema coelomaticum (Trematoda, Dicrocoeliidae) is a digenean flatworm found in ruminants that is the causative agent of eurytrematosis, a disease of veterinary health concern. In Brazil, morphological and molecular data indicate that *E. coelomaticum* is the only species parasitizing livestock (Travassos, 1944; Travassos *et al.*, 1969; Figueira *et al.*, 2014). The ultrastructural organization of *E. coelomaticum* cercariae, mother and daughter sporocysts (Franco-Acuña *et al.*, 2011; Pinheiro *et al.*, 2011, 2012), and eggs (Pinheiro *et al.*, 2015) has been investigated using scanning and transmission electron microscopies. Other works have already used advanced microscopy experiments for investigating nematodes (Adnet *et al.*, 2013; Lopes-Torres *et al.*, 2015), cestodes (Almeida *et al.*, 2015) and some trematode species (Machado-Silva *et al.*, 1998; Souza *et al.*, 2011, 2017; Gonçalves *et al.*, 2016; Marques *et al.*, 2017). Despite the excellent resolution to characterize the surface structures in detail, conventional scanning electron microscopies (SEMs) limit the observation to the external surfaces, missing information about the internal ones. Light microscopy (LM; brightfield and fluorescence) provides information about internal structures, being complemented by SEM and the cryofracture technique (Lopes-Torres *et al.*, 2019).

Currently, most studies on adults of *E. coelomaticum* are based on conventional LM (Travassos, 1944; Travassos *et al.*, 1969). Over recent years, new insights into the morphology and anatomy of parasitic helminths have been generated using advanced imaging technologies, like the fluorescence and confocal microscopies (CMs) associated with electron microscopy experiments (Faulwetter *et al.*, 2013). Fluorescence analysis of large parasites, such as helminths, was neglected until recent advances in fluorescence stereomicroscopy using structured

© Cambridge University Press 2020

CAMBRIDGE UNIVERSITY PRESS

illumination and light sheet fluorescence microscopy, thus opening up new possibilities for the study, with the entire body of helminths in freshly fixed and hydrated samples (Lopes-Torres *et al.*, 2019). These findings show the importance of the association of modern multidimensional techniques for the understanding of helminth morphofunctionality, highlighting the potential of fluorescence microscopy as the basis for other experiments in the parasitology area.

In the present study, different experiments were performed using a combined approach of brightfield LM, fluorescence microscopy, CM and SEM to explore whole and cryofractured samples. This investigation focused on the attachment structures (oral and ventral suckers), reproductive organs (male and female), tegument ultrastructure and excretory apparatus.

Material and methods

Parasite sources

The adult worms were collected from the pancreas of naturally infected cattle that were slaughtered in an industrial slaughterhouse (Matadouro Municipal de Barra Mansa), Barra Mansa, RJ, Brazil, 22°32′39″S, 44°10′17″W) according to the sanitary surveillance rules (Pinheiro *et al.*, 2015). The parasites were fixed by immersion in AFA solution(the mixture by glacial acetic acid 2%, formaldehyde 3% and 70º ethanol 95%) at room temperature. The parasites were confirmed as *E. coelomaticum* based on LM according to the size of the suckers and of the body (Travassos, 1944).

Morphological examination

Twenty-five fixed worms were stained and prepared for LM, stereomicroscopy (brightfield and fluorescence) and CM imaging, as previously described (Neves *et al.*, 1998; de Souza, 2011). Briefly, the worms were stained with hydrochloric carmine, dehydrated in a graded ethanol series, cleared with methyl salicylate and mounted on microscope slides with Canada balsam. LM was carried out using a light microscope (Eclipse 80i, Japan) coupled to a digital camera (Nikon DS-Ri1, Japan) at the Rio de Janeiro State University (UERJ), Brazil. The experiments using stereomicroscopy were performed at the Urogenital Research Unit, Department of Anatomy, at the Institute of Biology Roberto Alcantara Gomes, UERJ (Discovery V8, Zeiss, Germany) and in the National Center for Structural Biology and Bioimaging (CENABIO) at the Rio de Janeiro Federal University (UFRJ; Axio Zoom.V16, Zeiss, Germany). The whole-mounted voucher specimen was deposited in the Helminthological Collection of the Institute Oswaldo Cruz, Rio de Janeiro, Brazil, under the number 38879.

CM

Whole mounts were imaged using a Nikon C2 confocal microscope (Nikon Instruments, Inc., New York, USA), operating at 556 nm excitation, 573 nm emission and pinhole at 1.4 (de Souza, 2011), in the Confocal/Fluorescence Microscopy Laboratory at the Institute of Biology Roberto Alcantara Gomes, UERJ.

SEM

Ten specimens were processed for SEM based on a previous protocol (Lopes-Torres *et al.*, 2013) and some specimens were frozen and fractured following a simple methodology previously described (Adnet *et al.*, 2013). Briefly, samples were dehydrated in a graded ethanol series (70–100% Degree Gay Lussac) for 40 minutes at each step, critical-point dried in CO_2, mounted on metallic stubs and coated with gold (20–25 nm deposited). After assembly, the samples were examined using the scanning electron microscopes Jeol/EO1.0 (Jeol, Japan) at the Institute of Chemistry, UERJ, and Zeiss EVO-MA10 (Zeiss, Germany) at the CENABIO-UFRJ.

Results

Description

Based on 25 whole-mounted specimens collected from cattle in Brazil and stained with hydrochloric carmine, the morphological and morphometric data of *E. coelomaticum* were analysed (fig. 1a, b). Specimens had a total body length of 7.07 ± 1.24 (4.43–8.95) mm and width of 3.66 ± 0.69 (2.20–4.91) mm. LM showed the attachment structures (fig. 1a, b), the subterminal oral sucker (0.45–0.96 mm) and ventral sucker (0.46–0.88 mm) placed in the forebody. The pharynx was short (0.17–0.29 mm), and the oesophagus followed by two caeca branches. The male reproductive system showed two globular posterolateral testes and a well-developed elongated cirrus-sac, 1.23 ± 0.18 (0.95–1.66 mm), extending from the intestinal bifurcation to the ventral sucker region (fig. 1a, b). The female reproductive system showed ovaries with a diameter of 0.29 ± 0.08 (0.16–0.48) mm, The Mehlis' gland complex and the vitelline reservoir were positioned in the mid hindbody, posterior to the testes; the vitelline follicles were arranged in two lateral fields restricted to the mid hindbody; uterus with many brown eggs filling the hindbody, extending to the anterior region and overlapping the ventral sucker. The posterior region presented the excretory pore and eggs overlapping the excretory vesicle (fig. 1a, b). The fluorescence stereomicroscopy highlighted the cubic crystal protein inclusions (fig. 1b).

The tegument revealed a typical pattern of indentation of various sizes at irregular intervals (figs 1a, b and 2a). CM showed that the thickened-syncytial layer gives rise to the tegument indentation, invading the parenchyma area (fig. 2b). SEM revealed a spineless surface on the syncytial tegumental layer with a honeycomb pattern (fig. 2c).

The anterior region of the body is marked by the main fixation structures, the oral and ventral suckers (fig. 3a, b). Observed using SEM, the forebody of the adult worms presented a spineless tegument. The median genital pore was located between the suckers, while typical cubic crystal protein inclusions were originated and projected from the external syncytial layer (fig. 3b). The muscular organization was an important structure for the efficacy of the parasitic strategy, in which the suckers played a critical function in their attachment inside the hosts. Confocal examination revealed that the oral and ventral suckers presented a dense and complex arrangement of the muscle fibre system (fig. 3c–f). The oral and ventral sucker muscles were formed by strong radially arranged fibres overlapping circular, diagonal, transverse and longitudinal fibres (fig. 3c–f). Besides, this tool allowed the visualization of inner parenchymal cells and large cell nuclei around the oral sucker (fig. 3e) and cubic crystal proteins on the outer muscular fibres of the ventral sucker (fig. 3f). The pharynx is

https://doi.org/10.1017/S0022149X19001135 Published online by Cambridge University Press

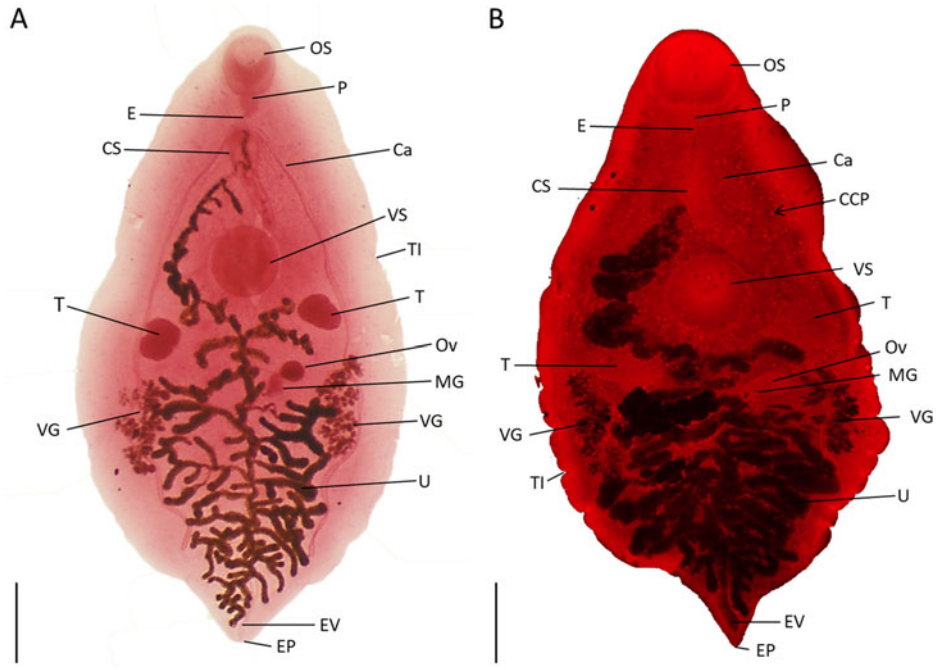


Fig. 1. Overview of *Eurytrema coelomaticum* adult worm collected from cattle in Rio de Janeiro State (Brazil). Whole-mounted specimen in ventral view showing internal and external structures. (A) Brightfield stereomicroscope; (B) fluorescence stereo zoom microscope. Scale bars: 500 µm. Abbreviations: Ca, caeca; CCP, cubic crystal protein inclusions; CS, cirrus-sac; E, oesophagus; EP, excretory pore; EV, excretory vesicle; MG, Mehlis' gland complex; OS, oral sucker; Ov, ovary; P, pharynx; T, testes; TI, tegument invagination; U, uterus; VS, ventral sucker; VG, vitelline gland.

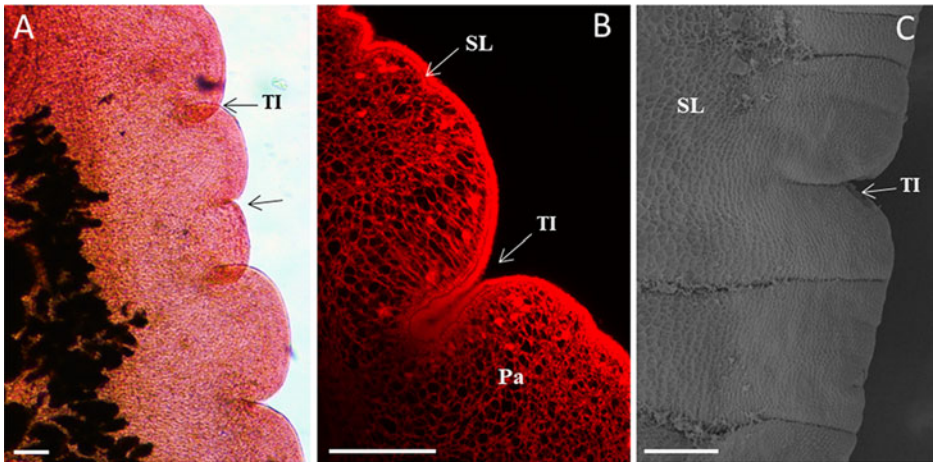


Fig. 2. External view of *Eurytrema coelomaticum* adult. (A) Light microscopy of the lateral surface showing (tegument indentation) irregularly distributed tegumental invagination; (B) confocal microscopy showing a thicker syncytial layer, which forms tegument indentation of various sizes, invading the parenchyma area; (C) scanning electron microscopy revealed spineless syncytial layer with a honeycomb pattern and tegument indentation. Scale bars: (A) 100 µm; (B, C) 50 µm. Abbreviations: Pa, pacrenchyma; SL, syncytial layer; TI, tegument identation.

an ellipsoid thick-walled organ (figs 3c, g, h) formed, to a large extent, by radial fibres being circumvented on its edges by external and internal longitudinal muscle fibres and presenting parenchymal cells with visible nuclei associated to the pharynx muscular structure (fig. 3g, h). The oesophagus was placed immediately posterior to the pharynx, being thick-walled with longitudinal fibres, with glandular cells around this area (figs 3c, g, h).

The internal view at the midbody level showed parenchymal cells with visible nuclei and muscle fibres with lower density than in the suckers, which were arranged in dense parenchyma that filled the parasite body (fig. 4a). Freeze-fracture and SEM assays have detailed the parenchymal cell distribution in the meshwork-like parenchyma (fig. 4b).

The whole-mounted specimens examined by LM showed the presence of a cirrus-sac in the forebody (fig. 5a) and the confocal experiments revealed its well-developed wall with a muscular opening to a genital pore (gonopore). The cirrus-sac encompasses the central S-shaped ejaculatory duct enveloped by a well-developed, thick-walled prostatic gland, connected to the seminal vesicle. There were numerous secretory cells external to the ejaculatory duct (fig. 5b). The lumen of the seminal vesicle was filled with spermatozoa (fig. 5c) and, as expected for sexually mature worms, glandular follicles and spermatozoa were visualized inside the testes (fig. 5d). The SEM cryofracture image showed a round-shaped testis with a smooth surface (fig. 5e), while ultrastructure has revealed that male worms present well-developed, extroverted cirrus with a smooth surface (fig. 5f). The scheme of the cirrus-sac was represented as follows: the anterior end represented the protractile cirrus, which emerged out of the gonopore; the genital atrium was small, receiving the female uterus from the left side, laterally, to the cirrus-sac; the ejaculatory duct widened posteriorly to form seminal vesicles filled with spermatozoa; and prostatic glands were densely distributed in the anterior region to the seminal vesicle, surrounding the ejaculatory duct (fig. 5g).

An overview of the whole-mounted worms showed the uterus filled with brown eggs extending from the posterior half of the

https://doi.org/10.1017/S0022149X19001135 Published online by Cambridge University Press

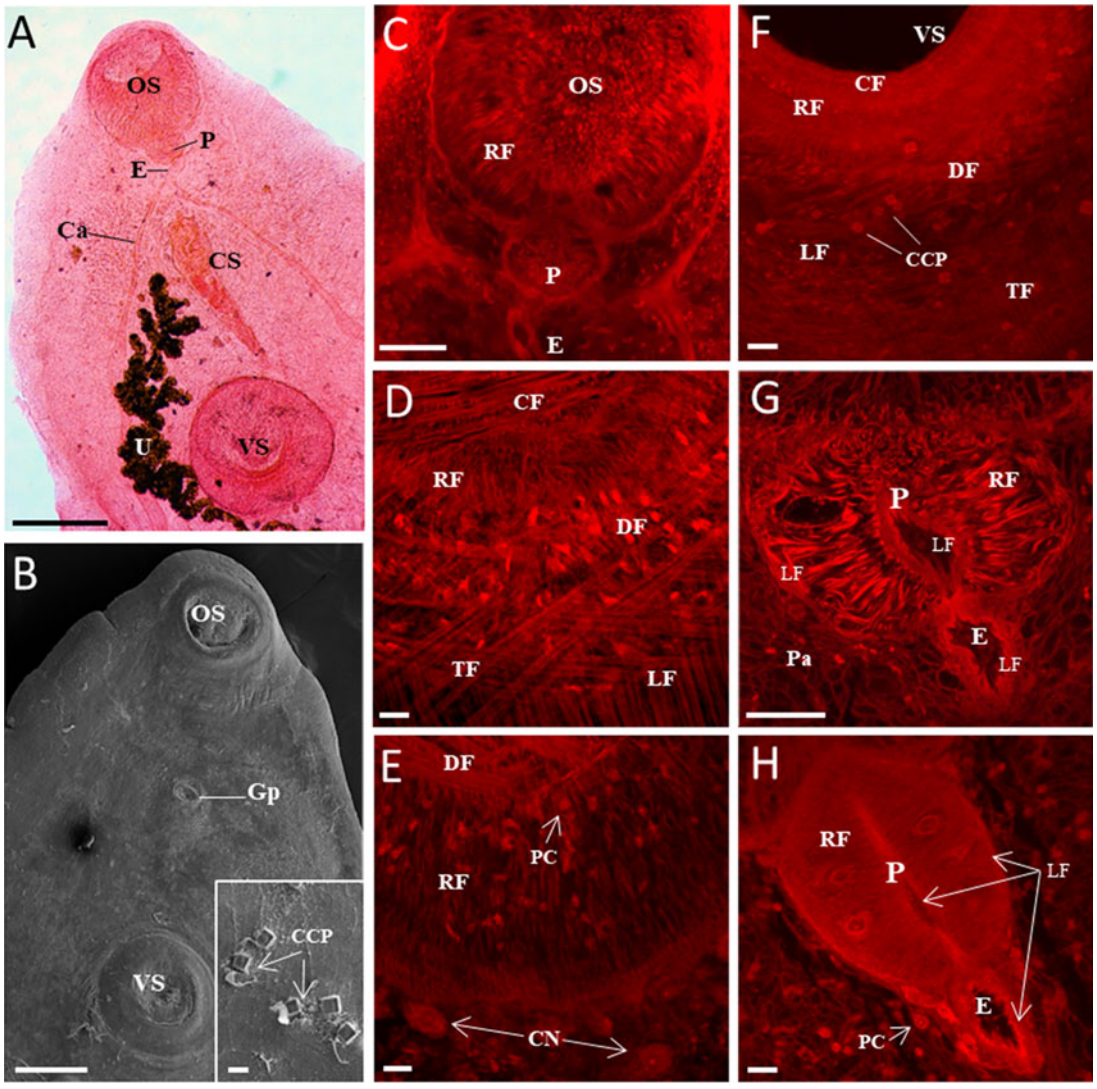


Fig. 3. *Eurytrema coelomaticum* forebody. (A) Brightfield showing attachment structures (oral and ventral suckers), digestive (pharynx, short oesophagus and intestinal bifurcation anterior to ventral sucker) and reproductive organs (cirrus and uterus filled with many brown eggs) in the forebody. (B) SEM images showing suckers and genital pore situated between the suckers and cubic crystal protein inclusions situated close to the ventral sucker (inset). (C–H) Confocal images showing typical arrangement of the complex system of the sucker and pharynx muscles. Circular, radial, diagonal transverse and longitudinal fibres within and around the oral sucker (C, D, E), ventral sucker (F) and pharynx (G, H). Parenchymal cells (arrow) and cell nuclei were detected inside the oral sucker (E). Scale bars: (A) 500 µm; (B) 200 µm (inset 20 µm); (D, E, H) 20 µm; (C) 100 µm; (F, G) 50 µm. Abbreviations: Ca, caeca; CCP, cubic crystal proteins inclusions; CF, circular fibres; CS, cirrus-sac; E, oesophagus; GP, gonopore; DF, diagonal fibres; LF, longitudinal fibres; CN, cell nucleus; OS, oral sucker; P, pharynx; Pa, parenchyma; RF, radial fibres; PC, parenchymal cells; TF, transverse fibres; U, uterus; VS, ventral sucker.

body to the mid-way between the genital pore and ventral sucker. Ovary was single, small, round and post-testicular; Mehlis' gland complex and vitelline glands were distributed in two lateral fields (fig. 6a). CM allowed the observation of the Laurer's canal, obscured by eggs, while LM enabled the identification of the intercecal uterus, vitelline reservoir, Mehlis' gland complex and vitelline duct (fig. 6a). Confocal examination resulted in more detailed images of the reproductive tracts such as the ovary, Mehlis' gland and cells inside the ootype (fig. 6b). As aforementioned, the Laurer's canal was darkened by eggs. Nevertheless, the CM showed its dense musculature organization (fig. 6c). Inside the ovary, numerous round oocytes were observed (fig. 6d). The scheme of the female reproductive organ is shown in fig. 6e. Oviduct emanating from a single ovary with oocytes, expanding in the proximal portion to form a seminal receptacle. A narrow tube (Laurer's canal) joins the tubular oviduct, together with the seminal receptacle and the vitelline reservoir, before oviduct joins the characteristic thick wall ootype, an expansion of the oviduct surrounded by numerous Mehlis' gland. This organ contributes to the eggshell formation. The developing eggs leave the ootype to the uterus, through which the eggs are transported to the exterior.

Intrauterine eggs were examined both by the CM and the freeze-fracturing technique (fig. 7). Eggs with thick shells were found in the loops of the uterus (fig. 7a). Eggs containing well-developed embryos were also present (fig. 7b) and images of the fractured eggs showed the eggs inside the uterine lumen in diverse stages of embryonic development (fig. 7c, d). Oval shape, presence of opercula and smooth surface (fig. 7d). In addition, mucus was found in this region, providing protection to the reproductive structures (fig. 7d).

An excretory pore and a slice excretory vesicle were visualized at the posterior end of the body (fig. 8a–c). LM revealed an

https://doi.org/10.1017/S0022149X19001135 Published online by Cambridge University Press

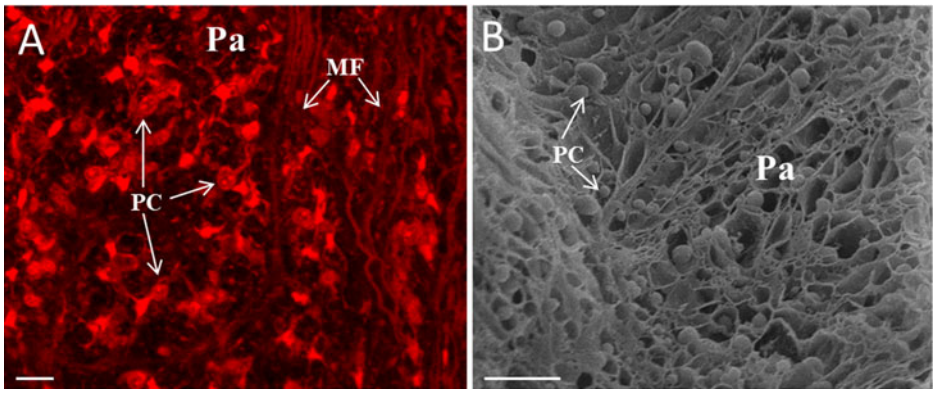


Fig. 4. Internal view of the midbody of *Eurytrema coelomaticum* adult. (A) Confocal microscopy image showing parenchymal cells and muscle fibres dispersed into the lacunar parenchyma; (B) cryofracture scanning electron microscopy images showing rounded parenchymal cells dispersed into the meshwork-like parenchyma. Scale bars: 20 µm. Abbreviations: MF, muscle fibres; Pa, parenchyma; PC, parenchymal cells.

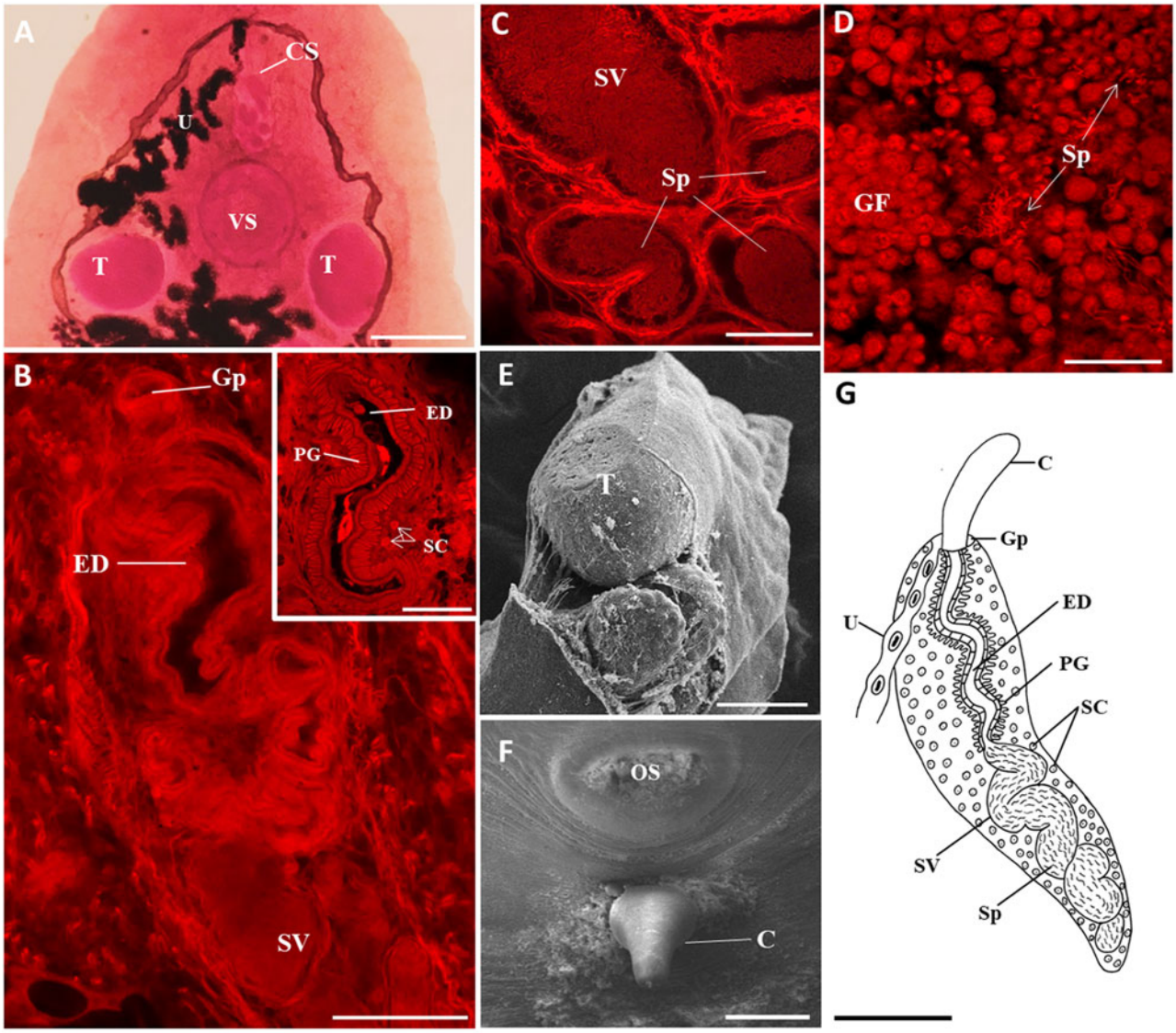


Fig. 5. Genitalia of *Eurytrema coelomaticum*. Ventral view. (A) Whole-mounted specimen observed with brightfield microscopy showing cirrus-sac and uterus; two elliptical nearly symmetrical testes posterior to ventral sucker. (B–D) All stained specimens were also analysed by confocal microscopy. (B) Imaging of cirrus-sac reproductive structures showing gonopore, thick-walled ejaculatory duct and tangled seminal vesicle. The white square details the same region, where secretory cells are also present. (C) Detail of internal seminal vesicle with abundant spermatozoa content. (D) Inside the testes, glandular follicles and spermatozoa were visualized. (E, F) Scanning electron microscopy. (E) Cryofracture image of a single round testis. (F) Image showing everted, conical, smooth cirrus close to the oral sucker. (G) Scheme showing cirrus, uterus with eggs opening at the level of the gonopore, cirrus-sac with ejaculatory duct, prostatic gland and enlarged prolongation of the ejaculatory duct forming seminal vesicle containing abundant spermatozoa. Scale bars: (A) 500 µm; (B) 100 µm (inset 50 µm); (C, D) 20 µm; (E–G) 200 µm. Abbreviations: C, cirrus; CS, cirrus-sac; ED, ejaculatory duct; GF, glandular follicles; GP, gonopore; OS, oral sucker; SC, secretory cells; SV, seminal vesicle; Sp, spermatozoa; T, testes; U, uterus; VS, ventral sucker.

https://doi.org/10.1017/S0022149X19001135 Published online by Cambridge University Press

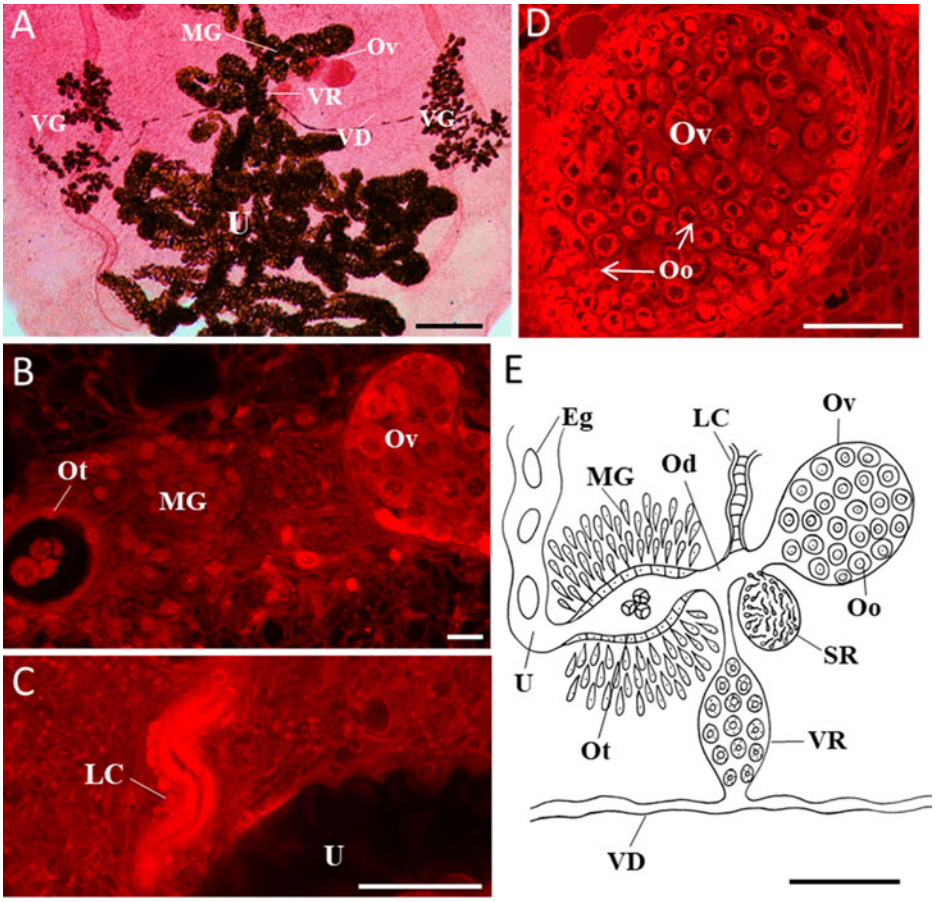


Fig. 6. Female genitalia of *Eurytrema coelomaticum*. Ventral view. (A) Whole-mounted specimen observed with brightfield microscopy showing a small single ovary, Mehlis' gland complex, vitelline reservoir, vitelline duct, vitelline glands in two lateral fields and thousands of brownish eggs within the uterus. (B–D) All stained specimens were also analysed by confocal microscopy. (B) Site of egg formation showing ovary and ootype surrounded by Mehlis' gland cells. (C) Thick-walled Laurer's canal and partial view of uterus. (D) Note oocytes within the ovary. (E) Scheme illustrating female genitals. Single ovary with oocytes. Laurer's canal joins the tubular oviduct together with the seminal receptacle and the vitelline reservoir. The oviduct expands in the proximal portion to form the ootype surrounded by Mehlis' gland cells. The uterus, containing eggs formed, originates at the level of the distal ootype. The vitelline reservoir extends by connecting to the vitelline glands through the vitelline ducts. Scale bars: (A) 500 μm; (B) 20 μm; (C, E) 100 μm; (D) 50 μm. Abbreviations: Eg, eggs; LC, Laurer's canal; MG, Mehlis' gland; Oo, oocyte; Ot, ootype; Od, oviduct; Ov, ovary; SR, seminal receptacle; U, uterus; VG, vitelline glands; VR, vitelline reservoir; VD, vitelline duct.

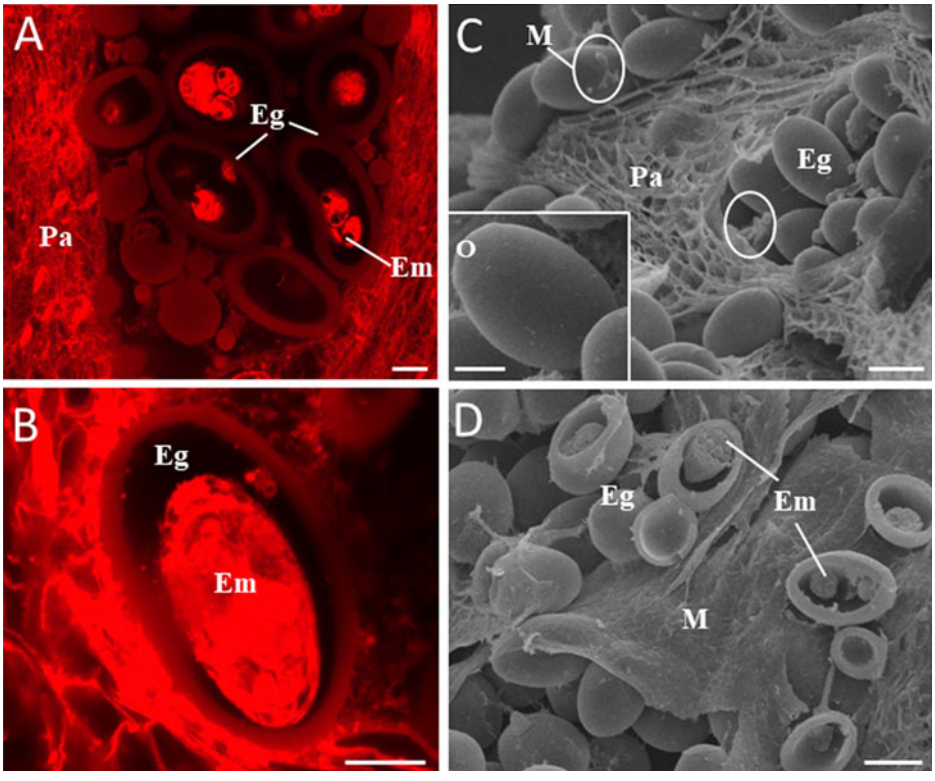


Fig. 7. Intrauterine eggs of *Eurytrema coelomaticum*. (A, B) Confocal microscopy of whole-mounted preparations. (A) Eggs with thick eggshell in the uterus. (B) A single egg with well-developed embryo. (C, D) SEM cryofracture images. (C) Eggshell-enclosing developing embryos in the uterine loops. Inset: note operculum on the anterior end and the apparently smooth tegument. (D) Several thick-shelled eggs in different stages of embryonic development and mucus. Scale bars: (A, B, D) 10 μm; (C) 100 μm (inset 10 μm). Abbreviations: Eg, eggs; Em, embryo; M, mucus; O, operculum; Pa, parenchyma.

https://doi.org/10.1017/S0022149X19001135 Published online by Cambridge University Press

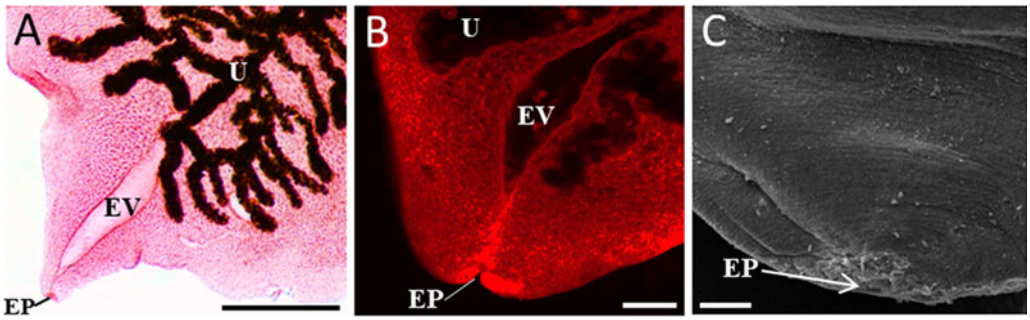


Fig. 8. Posterior region of *Eurytrema coelomaticum* adult. (A, B) Brightfield and confocal microscopies showing the uterus overlying the excretory vesicle and the excretory pore opening. (C) Scanning electron microscopy showing a smooth slightly depressed tegument around the excretory pore. Scale bars: (A) 500 µm; (B) 100 µm; (C) 20 µm. Abbreviations: EP, excretory pore; EV, excretory vesicle; U, uterus.

excretory terminal pore (fig. 8a). In addition, CM (fig. 8b) and SEM (fig. 8c) revealed the excretory pore opening, indicating the point of contact with the external environment.

Discussion

In recent years, there has been significant progress in microscopic technologies, leading to new insights into the morphology and anatomy of parasitic worms (Faulwetter *et al.*, 2013; Lopes Torres *et al.*, 2015; Gonçalves *et al.*, 2016; Conn *et al.*, 2018). Therefore, the current study aimed to provide new data about the external and internal organization of *E. coelomaticum* adults, based on a combination of advanced morphological experiments.

Cubic crystal protein inclusions are structures described in *E. coelomaticum* that probably represent a conservative character, since they were found in *E. coelomaticum* adults from different countries and were observed in detail using electron microscopy in specific regions of the body (Sakamoto & Oikawa, 2007). As expected, SEM images showed cubic crystal inclusions on the tegument surface. In addition, based on our fluorescence stereomicroscopy experiments, a wide distribution of these crystals was detected on the trematode body. There is evidence to support that these inclusions appear in the subtegumental region and are transported to the tegument along cytoplasmic bridges (Sakamoto & Oikawa, 2007). Our CM examination revealed that the crystal protein inclusions were also present at the level of the ventral sucker, representing the first report describing such structures by CM. Therefore, this investigation has reinforced the importance of CM to study the inner structures of parasitic flukes (Machado-Silva *et al.*, 1998; Šebelová *et al.*, 2004; Neves *et al.*, 2005, Souza *et al.*, 2017). It is likely that cubic crystal protein inclusions present a metabolic function because they were found in adult worms from different countries, showing that they are not associated with a specific condition, such as host diet, fixation or another artefact.

The gonopore is medially situated in the forebody between the suckers; the characteristics of the elongated cirrus-sac and testes herein described are consistent with previous descriptions (Travassos *et al.*, 1969; Pinto & de Melo, 2016). The confocal results revealed a well-developed cirrus-sac composed of a seminal vesicle, a well-developed prostatic gland and secretory cells surrounding the S-shaped ejaculatory duct, which ended in the cirrus exposed through the genital pore, as found in *Fasciola hepatica* and *Trichobilharzia regenti* (Terasaki *et al.*, 2001; Skírnisson *et al.*, 2012). In addition, SEM showed that both cirrus and testes have smooth margins, similar to the other Dicrocoeliidae species (Casanova & Ribas, 2004; Hildebrand *et al.*, 2007).

Although earlier LM-based studies (Travassos, 1944; Travassos *et al.*, 1969) have shown the lateral margin of *E. coelomaticum* adult, no information is currently available regarding its characterization. Confocal and SEM examination enabled us, for the first time, to show that it is composed of invaginations of various sizes at irregular intervals, as reported in digenean flatworm parasites of Brazilian catfishes (Cohen *et al.*, 2001).

Given that digenean trematodes utilize suckers for dislodging, attachment and feeding within their host tissues, the muscular organization of these suckers has attracted much interest, especially due to the increase of knowledge about the organization of the fibres that might be new targets for drugs (Kumar *et al.*, 2003; Krupenko, 2019). Consistent with previous investigations also using CM, a typical arrangement formed by diagonal, circular, radial, transverse and longitudinal (=meridional) muscle fibres was observed (Mair *et al.*, 1998; Kumar *et al.*, 2003, Šebelová *et al.*, 2004; Krupenko, 2014; Borges *et al.*, 2017; Krupenko, 2019). These types of muscle fibres may vary in organization and amount across different helminth groups, suggesting an evolutionary character associated with the behaviour of the parasite and the site they occupy within the host (Mair *et al.*, 2000; Krupenko & Dobrovolskij, 2015; Krupenko, 2019).

Previous works showed in detail the female reproductive system, and our results using LM have confirmed the morphological and morphometric patters presented in these classical descriptions (Travassos, 1944; Travassos *et al.*, 1969). Nevertheless, confocal images showed a single ovary filled with numerous oocytes, a conserved character among digenean trematodes (Neves *et al.*, 2005; Souza *et al.*, 2011; Hanna, 2015; Marques *et al.*, 2017), highlighting that reproductive efficiency is an important adaptation of the organisms to parasitic life. Laurer's canal is a structure present in digenean species. However, its detection is very difficult using only brightfield microscopy, mainly because of its overlapping position with the uterus. In the present study, the confocal series images have overcome this limitation, enabling us to detail the Laurer's canal, showing that it is a thick-walled tube (Bullard *et al.*, 2012; Skírnisson *et al.*, 2012; Womble *et al.*, 2015; Roberts *et al.*, 2016).

Limited data are currently available describing the egg-forming complex in *E. coelomaticum* (Pinheiro *et al.*, 2015). The present study has revealed that the ootype is surrounded by the Mehlis' gland, as previously shown for *F. hepatica* using transmission electron microscopy (Colhoun *et al.*, 1998) and for *Echinostoma paraensei* using CM (Souza *et al.*, 2011). Among digeneans, it is

https://doi.org/10.1017/S0022149X19001135 Published online by Cambridge University Press

well-established that egg formation takes place in a thick-walled chamber (ootype), where the eggshell is formed from material derived from the vitelline cells combined with secretions of the Mehlis' gland (Cogswell *et al.*, 2012).

Knowledge about the uterine development of *E. coelomaticum* eggs is scarce (Pinheiro *et al.*, 2015). As observed in the current confocal study, the uterus contains numerous thick-walled spherical-to-ellipsoid eggs, free within the uterine loops, as previously described (Pinheiro *et al.*, 2015). Over the last decade, the cryofracture technique has been proved a simple method used to prepare biological samples by exposing internal structures for visualization using SEM (Taylor, 2008). Indeed, previous studies have provided valuable new information about parasitic flukes (Adnet *et al.*, 2013). As mentioned above, in order to better characterize the uterine eggs observed by CM, a detailed examination using the cryofracture technique was performed. The main advantage was the visualization of embryos inside the maternal uterine tissues, which may greatly facilitate the analysis of the embryogenesis. This investigation has shown uterine eggs surrounded by mucus with embryo in different developmental stages (Conn *et al.*, 2018) and eggs with a well-defined operculum (Pinheiro *et al.*, 2015).

In recent years, increasing drug resistance worldwide has been observed in gastrointestinal helminths that parasitize livestock (Radio *et al.*, 2018). Hence, strategies are necessary to develop and test new and effective anthelmintic drugs (Srivastava & Misra-Bhattacharya, 2015). The detection of intrauterine eggs found in adult parasites, as performed in the present study, might also contribute to a better analysis of the action of relevant compounds on digenean flukes of human and veterinary importance, as determined by histology and light and electron microscopies (Hanna, 2015; Abdelaal *et al.*, 2016; Hanna *et al.*, 2016; Pereira *et al.*, 2016). Although a previous study has investigated the action of praziquantel and triclabendazole against *Eurytrema pancreaticum* adults (Jiraungkoorskul *et al.*, 2005), the treatment for *E. coelomaticum* remains unknown (Ilha *et al.*, 2005).

Brightfield microscopy has shown the body terminating into a terminal excretory pore at the posterior end of the body, although the anterior region of the excretory vesicle was hidden by the uterine eggs (Bray & Justine, 2013). However, detailed information on its morphology is limited. In our confocal results we have noted that the opening of the excretory pore presents a well-defined border and the SEM images enabled a detailed analysis of this structure, revealing a smooth tegument and depressions in the wrinkled body wall, as seen in other digenean flukes (Machado-Silva *et al.*, 1997; Maldonado *et al.*, 2003).

Considering the results mentioned above, this work has conclusively demonstrated that the combination of advanced morphological experiments might yield complementary data that are not provided by a single isolated technique. Thus, our understanding was enhanced about the structural organization of *E. coelomaticum* adult stages. Finally, this work contributes new morphological criteria to evaluate the effects of antiparasitic drugs on flukes of medical and veterinary importance.

Acknowledgements. The authors would like to thank Dr Jairo Pinheiro da Silva, Department of Physiological Sciences, Institute of Biology and Department of Animal Parasitology, Veterinary Institute, Federal Rural University of Rio de Janeiro, Seropédica, RJ, for providing the *Eurytrema* samples. Our thanks to the Department of Anatomy, Confocal Microscopy/Fluorescence Laboratory and Institute of Chemistry, Rio de Janeiro University State, and also to the National Center for Structural Biology and Bioimaging, Rio de Janeiro Federal University, for providing technical assistance.

Financial support. This work was supported by the Conselho Nacional de Desenvolvimento Científico e Tecnológico (CNPq) and Fundação Carlos Chagas Filho de Amparo à Pesquisa do Estado do Rio de Janeiro (FAPERJ). KGL received scholarship from Coordenação de Aperfeiçoamento de Pessoal de Nível Superior (CAPES); (JCNE E-26/202.660/2018).

Conflicts of interest. None.

References

Abdelaal MMO, Brennan GP, Abdel-Azi A and Fairweather I (2016) Ultrastructural changes to the tegumental system and gastrodermal cells of adult *Fasciola hepatica* following treatment *in vivo* with a commercial preparation of myrrh (Mirazid). *Journal of Helminthology* **91**, 672–685.

Adnet FA, Gonçalves JP, de Souza W and Attias M (2013) A simple and efficient method to observe internal structures of helminths by scanning electron microscopy. *Microscopy and Microanalysis* **19**, 1470–1474.

Almeida F, Oliveira F, Neves R, Siqueira N, Rodrigues-Silva R, Daipert-Garcia D and Machado-Silva JR (2015) Morphometric characteristics of the metacestode *Echinococcus vogeli* Rausch & Bernstein, 1972 in human infections from the northern region of Brazil. *Journal of Helminthology* **89**, 480–486.

Borges JN, Costa VS, Mantovani C, Barros E, Santos EG, Mafra CL and Santos CP (2017) Molecular characterization and confocal laser scanning microscopic study of *Pygidiopsis macrostomum* (Trematoda: Heterophyidae) parasites of guppies *Poecilia vivipara*. *Journal of Fish Diseases* **40**, 191–203.

Bray RA and Justine JL (2013) Bucephalidae (Digenea) from epinephelines (Serranidae: Perciformes) from the waters off New Caledonia, including *Neidhartia lochepintade* n. sp. *Parasite* **20**, 56.

Bullard SA, Williams Jr EH and Bunkley-Williams L (2012) New genus and species of fish blood fluke (Digenea: Aporocotylidae Odhner, 1912) from stoplight parrotfish, *Sparisoma viride* (Bonnaterre, 1788), (Labridae: Scarinae) in the Caribbean Sea. *Journal of Parasitology* **98**, 1139–1143.

Casanova JC and Ribas A (2004) Description of *Brachylecithum mackoi* n. sp. (Digenea: Dicrocoeliidae) from the *European hedgehog*, *Erinaceus europaeus* (Insectivora: Erinaceidae). *Journal of Parasitology* **90**, 793–796.

Cogswell AA, Kommer VP and Williams DL (2012) Transcriptional analysis of a unique set of genes involved in *Schistosoma mansoni* female reproductive biology. *PLoS Neglected Tropical Diseases* **6: e1907**.

Cohen SC, Kohn A and Baptista-Farias MDF (2001) Scanning and transmission electron microscopy of the Tegument of Paranaella luquei Kohn, Baptista-Farias & Cohen, 2000 (microcotylidae, monogenea), parasite of a Brazilian Catfish, Hypostomus regain. *Memórias do Instituto Oswaldo Cruz* **96**, 555–560.

Colhoun LM, Fairweather I and Brennan GP (1998) Observations on the mechanism of eggshell formation in the liver fluke, *Fasciola hepatica*. *Parasitology* **116**, 555–567.

Conn DB, Świderski Z and Miquel J (2018) Ultrastructure of digenean trematode eggs (Platyhelminthes: Neoophora): a review emphasizing new comparative data on four European Microphalloidea. *Acta Parasitologica* **63**, 1–14.

de Souza W (2011) *Técnicas microscopia eletrônica aplicadas às ciências biológicas*. 3rd edn. Rio de Janeiro, Sociedade Brasileira de Microscopia, 420 pp.

Faulwetter S, Vasileiadou A, Kouratoras M, Thanos D and Arvanitidis C (2013) Micro-computed tomography: introducing new dimensions to taxonomy. *Zookeys* **263**, 1–45.

Figueira GF, Oliveira VH, Taroda A, Alfieri & AA and Headley SA (2014) Molecular characterization of *Eurytrema coelomaticum* in cattle from Paraná, Brazil. *Revista Brasileira de Parasitologia Veterinária* **23**, 383–386.

Franco-Acuña DO, Pinheiro J, Oliveira-Menezes A, Brandolini SV, DaMatta RA and de Souza W (2011) Light and scanning electron microscopy of sporocysts of *Eurytrema coelomaticum* (Giard et Billet, 1892) Looss, 1907. *Veterinary Parasitology* **177**, 72–78.

https://doi.org/10.1017/S0022149X19001135 Published online by Cambridge University Press

Gonçalves JP, Oliveira-Menezes A, Maldonado Jr A, Carvalho TMU and de Souza W (2016) Ultrastructural and cytochemical characterization of T1 and T2 secretory bodies from the tegument of *Echinostoma paraensei*. *Micron* **80**, 59–65.

Hanna REB (2015) *Fasciola hepatica*: histology of the reproductive organs and differential effects of triclabendazole on drug-sensitive and drug-resistant fluke isolates and on flukes from selected field cases. *Pathogens* **4**, 431–456.

Hanna REB, Moffetta D, Forstera FI, Trudgettb AG, Brennanb GP and Fairweatherb I (2016) *Fasciola hepatica*: a light and electron microscope study of the ovary and of the development of oocytes within eggs in the uterus provides an insight into reproductive strategy. *Veterinary Parasitology* **221**, 93–103.

Hildebrand J, Okulewicz J and Popiolek M (2007) A new dicrocoeliid from the bank vole *Clethrionomys glareolus* (Rodentia: Microtidae) from Poland. *Journal of Parasitology* **93**, 151–154.

Ilha MR, Loretti AP and Reis AC (2005) Wasting and mortality in beef cattle parasitized by *Eurytrema coelomaticum* in the State of Paraná, Southern Brazil. *Veterinary Parasitology* **133**, 49–60.

Jiraungkoorskul W, Sahaphong S, Tansatit T, Kangwanrangsan N and Pipatshukiat S (2005) *Eurytrema pancreaticum*: the *in vitro* effect of praziquantel and triclabendazole on the adult fluke. *Experimental Parasitology* **111**, 172–177.

Krupenko DY (2014) Muscle system of *Diplodiscus subclavatus* (Trematoda: Paramphistomida) cercariae, pre-ovigerous, and ovigerous adults. *Parasitology Research* **113**, 941–952.

Krupenko DY (2019) Oral sucker in Digenea: structure and muscular arrangement. *Zoomorphology* **138**, 29–37.

Krupenko DY and Dobrovolskij AA (2015) Somatic musculature in trematode hermaphroditic generation. *BMC Evolutionary Biology* **15**, 189.

Kumar D, McGeown JG, Reynoso-Ducoing O, Ambrosio JR and Fairweather I (2003) Observations on the musculature and isolated muscle fibres of the liver fluke, *Fasciola hepatica*. *Parasitology* **127**, 457–473.

Lopes-Torres EJ, de Souza W and Miranda K (2013) Comparative analysis of *Trichuris muris* surface using conventional, low vacuum, environmental and field emission scanning electron microscopy. *Veterinary Parasitology* **196**, 409–416.

Lopes-Torres EJ, Maldonado Jr A, Anjos DH, de Souza W and Miranda K (2015) Redescription of *Spirura guianensis* (Nematoda: Spiruridae) from a rare South American Gracile Opossum. *Acta Tropica* **150**, 87–93.

Lopes-Torres EJ, Girard-Dias W, Mello WN, Simoes RO, Pinto IS, Maldonado Jr A, de Souza W and Miranda K (2019) Taxonomy of *Physaloptera mirandai* (Nematoda: Physalopteroidea) based in three-dimensional microscopy and phylogenetic positioning. *Acta Tropica* **195**, 115–126.

Machado-Silva JR, Lanfredi RM and Gomes DC (1997) Morphological study of adult male worms of *Schistosoma mansoni* Sambon, 1907 by scanning electron microscopy. *Memórias do Instituto Oswaldo Cruz* **92**, 647–653.

Machado-Silva JR, Pelajo-Machado M, Lenzi HL and Gomes DC (1998) Morphological study of adult male worms of *Schistosoma mansoni* Sambon, 1907 by confocal laser scanning microscopy. *Memórias do Instituto Oswaldo Cruz* **93**, 303–307.

Mair GR, Maule AG, Shaw C and Halton DW (1998) Muscling in on parasitic flatworms. *Parasitology Today* **14**, 73–76.

Mair GR, Maule AG, Day TA and Halton DW (2000) A confocal microscopical study of the musculature of adult *Schistosoma mansoni*. *Parasitology* **121**, 163–170.

Maldonado Jr A, Vieira GO and Lanfredi RM (2003) *Echinostoma luisreyi* n. sp. (Platyhelminthes: Digenea) by light and scanning electron microscopy. *Journal of Parasitology* **89**, 800–808.

Marques JS, Rocha BM, Manso PPA and D'Ávila S (2017) New insights on the morphology of a digenean parasite (Digenea: Brachylaimidae, *Brachylaima mazzantii* (Travassos, 1927) using confocal laser scanning microscopy. *Zoosystema* **39**, 449–462.

Neves RH, Pereira MJ, de Oliveira RM, Gomes DC and Machado-Silva JR (1998) *Schistosoma mansoni* Sambon, 1907: morphometric differences between adult worms from sympatric rodent and human isolates. *Memórias do Instituto Oswaldo Cruz* **93**, 309–312.

Neves RH, de Lamare BC, Machado-Silva JR, Carvalho JJ, Branquinho TB, Lenzi HL, Hulstijn M and Gomes DC (2005) A new description of the reproductive system of *Schistosoma mansoni* (Trematoda: Schistosomatidae) analyzed by confocal laser canning microscopy. *Parasitology Research* **95**, 43–49.

Pereira CAJ, Oliveira LLS, Coaglio AL, Santos FSO, Cezar RSM, Mendes T, Oliveira FLP, Conzensa G and Lima WS (2016) Anti-helminthic activity of *Momordica charantia* L. against *Fasciola hepatica* eggs after twelve days of incubation *in vitro*. *Veterinary Parasitology* **15**, 160–166.

Pinheiro J, Franco-Acuña DO, Oliveira-Menezes A, Brandolini SV, de Souza W and DaMatta RA (2011) Ultrastructure of the sporocysts of *Eurytrema coelomaticum* (Giard Et Billet, 1892) Looss, 1907. *Veterinary Parasitology* **182**, 201–212.

Pinheiro J, Franco-Acuña DO, Oliveira-Menezes A, Brandolini SV, DaMatta RA and de Souza W (2012) New insight into the morphology of *Eurytrema coelomaticum* (Trematoda, Dicrocoeliidae) cercariae by light, scanning, and transmission electron microscopies. *Parasitology Research* **111**, 1437–1445.

Pinheiro J, Fanco-Acuña DO, Oliveira-Menezes A, Brandolini SVPB, Adnet FAO, Lopes Torres EJ, Miranda FJB, de Souza W and DaMatta RA (2015) Additional study of the morphology of eggs and miracidia of *Eurytrema coelomaticum* (Trematoda). *Helminthologia* **52**, 244–251.

Pinto HA and de Melo AL (2016) Comments on human eurytremiasis in Brazil. *World Journal of Experimental Medicine* **6**, 55–57.

Radio S, Fontenla S, Solana V, *et al.* (2018) Pleiotropic alterations in gene expression in Latin American *Fasciola hepatica* isolates with different susceptibility to drugs. *Parasite Vectors* **11**, 56.

Roberts JR, Orelis-Ribeiro R, Dang BT, Halanych KM and Bullard SA (2016) Blood flukes of Asiatic softshell turtles: revision of *Coeuritrema* Mehra, 1933 (Digenea: Schistosomatoidea) and a new species infecting Chinese softshell turtles, *Pelodiscus sinensis* (Trionychidae), from Vietnam. *Folia Parasitologica* **6**, 63.

Sakamoto T and Oikawa T (2007) Cubic crystal protein inclusions in the neodermis of the pancreatic fluke, *Eurytrema pancreaticum* and *Eurytrema coelomaticum*. *Parasitology Research* **101**, 1393–1399.

Šebelová S, Stewart MT, Mousley A, Fried B, Marks NJ and Halton DW (2004) The musculature and associated innervation of adult and intra molluscan stages of *Echinostoma caproni* (Trematoda) visualised by confocal microscopy. *Parasitolology Research* **93**, 196–206.

Skírnisson K, Kolářová L, Horák P, Ferté H and Jouet D (2012) Morphological features of the nasal blood fluke *Trichobilharzia regenti* (Schistosomatidae, Digenea) from naturally infected hosts. *Parasitology Research* **110**, 1881–1892.

Souza JGR, Garcia JS, Manso PPA, Neves RH, Maldonado Jr A and Machado-Silva JR (2011) Development of the reproductive system of the *Echinostoma paraensei* in *Mesocricetus auratus* analyzed by light and confocal scanning laser microscopy. *Experimental Parasitology* **128**, 341–346.

Souza JGR, Garcia JS, Gomes APN, Machado-Silva JR and Maldonado Jr A (2017) Comparative pattern of growth and development of *Echinostoma paraensei* (Digenea: Echinostomatidae) in hamster and Wistar rat using light and confocal laser canning microscopy. *Experimental Parasitology* **183**, 41–49.

Srivastava M and Misra-Bhattacharya S (2015) Overcoming drug resistance for macro parasites. *Future Microbiology* **10**, 1783–1789.

Taylor J (2008) Cryofracture or freeze-fracture, a method to expose internal tissue surfaces and cell surfaces for viewing in the scanning electron microscope. *Microscopy Today* **16**, 56–58.

Terasaki K, Itagaki T, Shibahara T, Noda Y and Moriyama-Gonda N (2001) Comparative study of the reproductive organs of Fasciola Groups by Optical Microscope. *Journal of Veterinary Medical Science* **63**, 735–742.

Travassos L (1944) Revisão da família Dicrocoeliidae, Odhner, 1910. *Monografias do Instituto Oswaldo Cruz*. **2**, 1–357.

Travassos L, Teixeira JF and Kohn A (1969) Trematódeos do Brasil. *Memórias do Instituto Oswaldo Cruz* **67**, 1–886.

Womble MR, Cox-Gardiner SJ, Cribb TH and Bullard SA (2015) First record of *Transversotrema* Witenberg, 1944 (Digenea) from the Americas, with comments on the taxonomy of *Transversotrema patialense* (Soparkar, 1924) Crusz and Sathananthan, 1960, and an updated list of its hosts and geographic distribution. *Journal of Parasitology* **101**, 717–725.

https://doi.org/10.1017/S0022149X19001135 Published online by Cambridge University Press